Absence of Integrin αvβ3 Enhances Vascular Leak in Mice by Inhibiting Endothelial Cortical Actin Formation

George Su[1], Amha Atakilit[1], John T. Li[1], Nanyan Wu[1], Mallar Bhattacharya[1], Jieling Zhu[1], Jennifer E. Shieh[1], Elizabeth Li[1], Robert Chen[1], Stephen Sun[1], Cynthia P. Su[1], and Dean Sheppard[1]

[1]Lung Biology Center, University of California San Francisco, San Francisco, California

Rationale: **Sepsis and acute lung injury (ALI) have devastatingly high mortality rates. Both are associated with increased vascular leak, a process regulated by complex molecular mechanisms.**

Objectives: **We hypothesized that integrin αvβ3 could be an important determinant of vascular leak and endothelial permeability in sepsis and ALI.**

Methods: **β3 subunit knockout mice were tested for lung vascular leak after endotracheal LPS, and systemic vascular leak and mortality after intraperitoneal LPS and cecal ligation and puncture. Possible contributory effects of β3 deficiency in platelets and other hematopoietic cells were excluded by bone marrow reconstitution experiments. Endothelial cells treated with αvβ3 antibodies were evaluated for sphingosine-1 phosphate (S1P)–mediated alterations in barrier function, cytoskeletal arrangement, and integrin localization.**

Measurements and Main Results: **β3 knockout mice had increased vascular leak and pulmonary edema formation after endotracheal LPS, and increased vascular leak and mortality after intraperitoneal LPS and cecal ligation and puncture. In endothelial cells, αvβ3 antibodies inhibited barrier-enhancing and cortical actin responses to S1P. Furthermore, S1P induced translocation of αvβ3 from discrete focal adhesions to cortically distributed sites through Gi- and Rac1-mediated pathways. Cortical αvβ3 localization after S1P was decreased by αvβ3 antibodies, suggesting that ligation of the αvβ3 with its extracellular matrix ligands is required to stabilize cortical αvβ3 focal adhesions.**

Conclusions: **Our studies identify a novel mechanism by which αvβ3 mitigates increased vascular leak, a pathophysiologic function central to sepsis and ALI. These studies suggest that drugs designed to block αvβ3 may have the unexpected side effect of intensifying sepsis- and ALI-associated vascular endothelial leak.**

Keywords: vascular endothelium; sepsis; acute lung injury; integrin

AT A GLANCE COMMENTARY

Scientific Knowledge on the Subject

Increased vascular leak is a central pathophysiologic feature of sepsis and acute lung injury, but the mechanisms governing this response remain unclear.

What This Study Adds to the Field

Integrin αvβ3 deficiency and blockade in mice increases the intensity of vascular leak in models of experimental acute lung injury and sepsis. αvβ3 blockade disrupts endothelial effects of sphingosine-1 phosphate, suggesting that αvβ3 plays a role in enhancing endothelial barrier function.

Sepsis and acute lung injury (ALI) are associated with high mortality rates and worldwide healthcare burden (1–4). Development of these syndromes requires complex host responses involving multiple cell types, inflammatory mediators, and coagulation factors. One pathophysiologic hallmark common to both sepsis and ALI is increased vascular leak. Increased vascular leak in sepsis leads to redistribution of intravascular fluid to extravascular compartments, hypovolemia, hemoconcentration, and stasis of blood flow. In ALI, alveolar spaces become flooded with pulmonary edema, resulting in impaired gas exchange, arterial hypoxemia, and respiratory failure (4–6).

It is generally believed that increased paracellular passage of solutes through the vascular endothelium occurs during acute inflammatory states (7, 8). Frequently cited models suggest that paracellular gaps form because of disrupted homeostasis between cytoskeletal, adhesive cell–cell, and cell–matrix forces (8–10). Integrins, a large family of heterodimeric glycoprotein receptors, are important mediators of these cellular functions and have been shown to participate in regulation of endothelial barrier function (11–13).

Integrin αvβ3 is expressed on almost all cells of mesenchymal origin, including several cell types contained within the vasculature: endothelial cells, smooth muscle cells, fibroblasts, leukocytes, and platelets. It binds to multiple ligands, including vitronectin, fibronectin, osteopontin, fibrinogen, and von Willebrand factor through interaction with the Arg-Gly-Asp motif (14, 15). Arg-Gly-Asp–containing peptides, which inhibit multiple members of the integrin family, have been shown to increase permeability in endothelial cell monolayers and in isolated intact coronary venules (16, 17).

β3 subunit knockout (KO) mice have increased dermal blood vessel leak in response to vascular endothelial growth factor (VEGF). This effect has been attributed to increased endothelial cell expression of VEGF receptor 2 (Flk-1) and thus exaggerated endothelial responses to VEGF (18, 19). The relevance, however, of β3 deficiency in models of clinical vascular leak has not been studied.

We report that β3 KO mice have increased mortality and systemic vascular leak after intraperitoneal LPS and cecal ligation and puncture (CLP) and increased lung vascular leak after endotracheal LPS. *In vivo* blockade of VEGF after intraperitoneal LPS had no effect on increased mortality in β3 KO mice, and expression levels of Flk-1 between β3 KO and wild-type

(*Received in original form August 2, 2011; accepted in final form September 26, 2011*)

Supported by NHLBI HL083950 (D.S.) and 1K08HL083097-01A1 (G.S.).

Author Contributions: conception and design, G.S. and D.S.; data acquisition, G.S., A.A., J.T.L., J.Z., J.E.S., E.L., R.C., S.S., and C.P.S.; analysis and interpretation, G.S., J.T.L., M.B., and D.S.; and drafting the manuscript for important intellectual content, G.S. and D.S.

Correspondence and requests for reprints should be addressed to George Su, M.D., Lung Biology Center, UCSF, 1550 4th Street, Room 545, San Francisco, CA 94121. E-mail: george.su@ucsf.edu

This article has an online supplement, which is accessible from this issue's table of contents at www.atsjournals.org

Am J Respir Crit Care Med Vol 185, Iss. 1, pp 58–66, Jan 1, 2012

Originally Published in Press as DOI: 10.1164/rccm.201108-1381OC on October 6, 2011
Internet address: www.atsjournals.org

mouse endothelial cells were similar after endotracheal LPS, suggesting that our findings were not specific to VEGF. Possible confounding effects of β3-deficiency in hematopoietic-derived cells in the intraperitoneal LPS model were excluded with bone marrow reconstitution experiments. In human endothelial cells, αvβ3 blocking antibodies increased their permeability response to multiple agonists including transforming growth factor (TGF)-β and thrombin, in addition to VEGF. These data suggest that αvβ3 contributes to a common downstream pathway that normally resists increases in endothelial permeability.

Sphingosine-1 phosphate (S1P), a potent phospholipid angiogenic factor released by activated platelets, has been shown to enhance endothelial barrier resistance (20, 21). Administration of S1P to animals in LPS- and ventilator-induced ALI is protective against vascular leak (22, 23). S1P-induced endothelial barrier enhancement requires signaling through the $S1P_1$ G-protein–coupled receptor (24), activation of Gi, and Rac1 guanosine triphosphatase (GTPase)–dependent formation of cortical actin (21). S1P regulates several other processes relevant to endothelial biology, and some effects, including endothelial cell migration and morphogenesis, have been shown to be dependent on αvβ3 (25).

In this study, we have identified αvβ3 as a novel modulator of S1P-induced endothelial barrier enhancement. S1P-induced barrier enhancement was inhibited by αvβ3 antibodies and was associated with Gi- and Rac1-dependent translocation of αvβ3 to cortical focal adhesions. These cortical focal adhesions were associated with S1P-induced cortical actin and seemed to require αvβ3 ligation for stabilization at cortical sites. Rac1 activation was not affected by αvβ3 antibodies, suggesting that effects modulated by αvβ3 are downstream of Rac1 signaling pathways. Taken together, our data suggest that αvβ3 mitigates vascular leak that contributes to sepsis syndrome and ALI, and that this function is dependent on αvβ3-mediated endothelial barrier enhancement.

METHODS

129/sv β3 Subunit KO and Wild-type Mice

β3 KO mice were a generous gift of Richard Hynes (Massachusetts Institute of Technology, Cambridge, MA). All experiments used age-matched female mice weighing 22 ± 3 g under guidelines approved by the University of California San Francisco Institutional Animal Care and Use Committee.

Reagents

See the online supplement for information.

Antibodies

See the online supplement for information.

Endotracheal LPS Model

See the online supplement for information.

Lung Evans Blue Extravasation Assay

See the online supplement for information.

Pulse Oximetry

Five consecutive sustained readings for at least 30 seconds were averaged using the MouseOx system (Starr Life Sciences, Oakmont, PA).

Primary Lung Endothelial Cells

Mouse lungs were perfused to clear, harvested *en bloc*, minced, and digested for 25 minutes in Liberase enzyme (28 Wünsch units/ml EBM-2 media). Cells were separated, labeled, and analyzed with an LSRII Flow cytometer (BD, Franklin Lakes, NJ) and Flowjo v. 7.5.4 software (Tree Star, Inc., Ashland, OR).

LPS Sepsis Model

See the online supplement for information.

Organ Extravascular Permeability Assay

Thirty-six hours after intraperitoneal LPS, I^{125}–bovine serum albumin was administered (0.5 μCi intravenously retroorbital). After 2 hours the mice were killed and organs harvested *en bloc*. I^{125}–bovine serum albumin tracer accumulation was measured as I^{125} counts per minute (Wizard γ counter; Perkin-Elmer, Waltham, MA).

Fluorescein Isothiocyanate–Dextran Localization of Mesenteric Plasma Leakage

Thirty-six hours after intraperitoneal LPS administration, fluorescein isothiocyanate (FITC)–labeled dextran was administered (60 mg/kg intravenously retroorbital). After 2 hours, mesentery whole mounts were prepared and fixed with 4% paraformaldehyde (26). FITC extravasation was imaged using a Leica DM5000B microscope (JH Technologies, San Jose, CA).

Quantification of VEGF-induced Vascular Leak

See the online supplement for information (13).

Bone Marrow Reconstitution

The protocol is courtesy of Shaun Coughlin (University of California San Francisco, San Francisco, CA) (*see* online supplement).

Mouse Platelet Isolation and Assessment of β3 Expression

The protocol is courtesy of Sanford Shattil (University of California San Diego, San Diego, CA) (*see* online supplement).

CLP Sepsis Model

See the online supplement for information (27).

Cell Adhesion Assay

See the online supplement for information.

Cell Culture

See the online supplement for information.

Assay of Transendothelial Albumin Flux

See the online supplement for information.

Immunocytochemistry Epifluorescence and Total Internal Reflection Fluorescence Imaging

Cells were grown on gelatin (0.1%)-coated glass coverslips to confluence over 15–20 hours. The cells were serum-starved and pretreated with antibodies for 1 hour, followed by agonists as described. The cells were then fixed with 4% paraformaldehyde, permeabilized with 0.5% triton X-100, labeled, mounted in 4',6-diamidino-2-phenylindole–Fluoromount-G, and imaged using a Leica DM5000B microscope equipped for epifluorescence (JH Technologies, San Jose, CA) or a Nikon TE2000 Inverted microscope equipped for total internal reflection fluorescence (TIRF) (Nikon Instruments U.S.A., Melville, NY). All images were processed with ImagePro software (Media Cybernetics, Inc., Bethesda, MD) or NIS Elements (Nikon Instruments U.S.A.).

DN Rac1 Adenovirus

See the online supplement for information.

Rac1 Activation Assay

See the online supplement for information.

Cortical αvβ3 Staining Intensity Analysis

TIRF images were analyzed using an intensity histogram function to identify the image panel normalization factor (minimum intensity).

Pixel bitmap intensity was mapped in 40 circular areas of interest (250-pixel area each) applied to cortical cell–cell junction sites. Maximum pixel intensity for each area of interest was recorded. Normalized intensity equals mean of maximum pixel intensities per areas of interest per minimum field pixel intensity. Analysis technicians were masked to panel identity. Images were processed with ImagePro software (Media Cybernetics, Inc.).

RESULTS

β3 KO Mice Have Increased Lung Vascular Leak after Endotracheal LPS

β3 KO mice had significantly increased lung vascular leak compared with wild-type controls after endotracheal LPS (Figure 1A) (28). This effect was also manifest as increased arterial hypoxemia in β3 KO mice (Figure 1B).

β3 KO mice have increased VEGF-induced dermal vascular leak, an effect ascribed to increased endothelial cell expression of VEGF receptor II (Flk-1) associated with β3 deficiency, and thus increased sensitivity to VEGF-induced effects (18, 19). We therefore measured Flk-1 expression on lung endothelial cells to assess for similar differential Flk-1 expression. However, significant differences in Flk-1 expression between cells isolated from β3 KO and wild-type mice were not found (Figures 1C and 1D). Flk-1 expression was measured immediately after endothelial cell isolation rather than from cells grown in primary culture (18, 19), which may account for the discrepancy between those published results and ours. Our data suggest that increased lung vascular leak seen in β3 KO mice is not likely caused by differences in VEGF signaling.

Previous studies have reported a wide range of endothelial αvβ3 expression levels, from altogether undetectable, to constitutively present in quiescent blood vessels, to very highly expressed in proliferating vessels during angiogenesis (29–31). We characterized lung endothelial cell expression of β3 and found that cells isolated from vehicle control-treated wild-

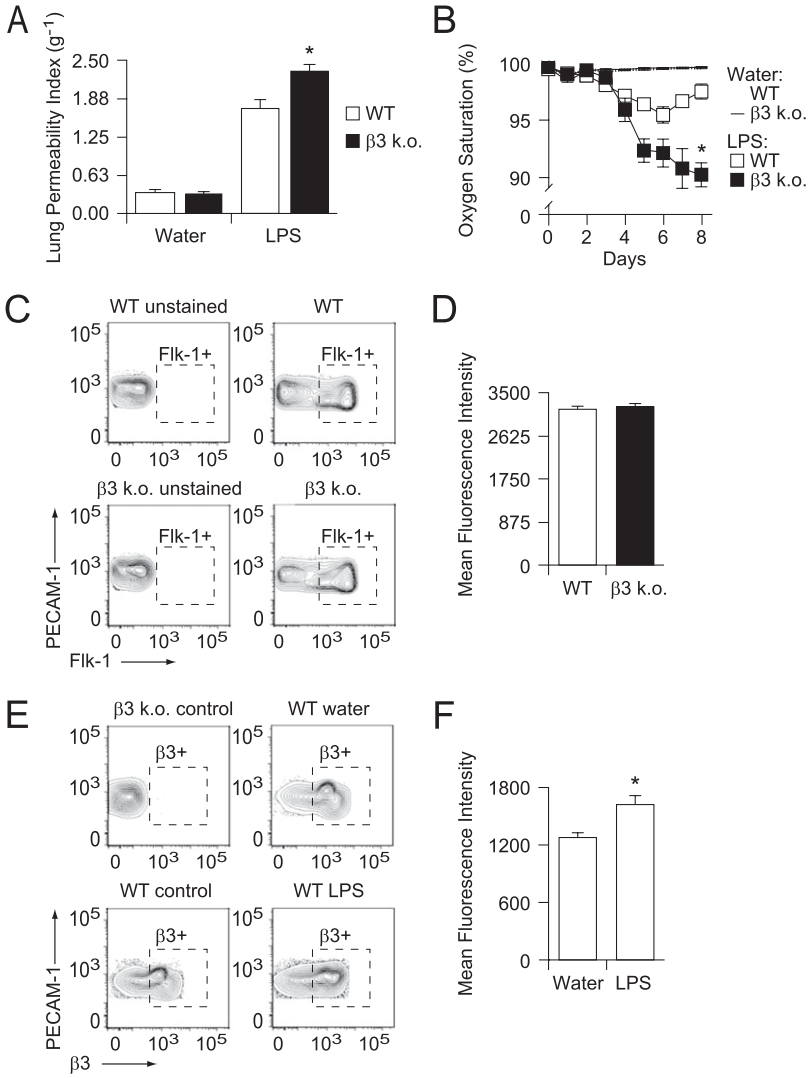

Figure 1. (*A*) β3 knockout (KO) mice have increased lung vascular leak after endotracheal LPS-induced acute lung injury. β3 KO and wild-type (WT) mice received LPS (200 μg in 50 μl water) or water control by endotracheal instillation. Extravasation of an intravascular Evans blue tracer into the lungs was measured at 8 days. The lung permeability index is expressed as lung extract/serum spectrophotometry absorbance units (620 nm) per dry weight of total lung (g^{-1}). Data shown are the means ± standard errors, n = 10 mice per group. *$P = 0.007$ for LPS-treated WT versus LPS-treated β3 KO mice. (*B*) β3 KO mice have increased arterial hypoxemia after endotracheal LPS-induced acute lung injury. After endotracheal instillation of LPS (200 μg in 50 μl water) or water control, daily pulse oximetry was performed. Reported values represent the average of five consecutive measurements that were sustained for at least 30 seconds. Data shown are the means ± standard errors, n = 10 mice per group. *$P = 0.016$ for LPS-treated WT versus LPS-treated β3 KO mice at 8 days. (*C* and *D*) Vascular endothelial growth factor receptor II (Flk-1) expression is equivalent in β3 KO and WT lung endothelial cells. (*C*) Lung cells from untreated β3 KO and WT mice were enzymatically liberated and labeled with dye-conjugated antibodies specific for platelet endothelial cell adhesion molecule (PECAM)-1, FcγRII and III, Gr-1, and Flk-1, and a live–dead marker. The cells were analyzed by flow cytometry and gated for live cells, against FcγRII and III and Gr-1 expression, and for PECAM-1. The resultant population was analyzed for Flk-1. β3 KO and WT cells not incubated with Flk-1 antibodies served as unstained controls. Representative contour plots of Flk-1 versus PECAM-1 expression are shown with outliers. *y* axis = PECAM-1 expression (mean fluorescence intensity); *x* axis = Flk-1 expression (mean fluorescence intensity). (*D*) Mean fluorescence intensity of Flk-1 expression in PECAM-1–expressing β3 KO and WT cells (gate Flk-1+ outlined with *dashed box* in *C*). Data shown are the means ± standard errors, n = 10 individual mouse samples per group, $P = 0.560$ for WT versus β3 KO mouse lung PECAM-1+ cells. (*E* and *F*) β3 expression is increased in lung endothelial cells after endotracheal LPS. (*E*) After endotracheal instillation of LPS (200 μg in 50 μl water) or water control, lungs cells were enzymatically liberated and labeled with dye-conjugated antibodies specific for PECAM-1, FcγRII and III, Gr-1, and β3, and a live–dead marker. The cells were analyzed by flow cytometry and gated for live cells, against FcγRII and III and Gr-1 expression, and for PECAM-1. The resultant population was analyzed for β3 expression. Cells isolated from untreated β3 KO and WT mice served as controls. Representative contour plots of β3 versus PECAM-1 expression are shown with outliers. *y* axis = PECAM-1 expression (mean fluorescence intensity), *x* axis = β3 expression (mean fluorescence intensity). (*F*) Mean fluorescence intensity of β3 expression in PECAM-1–expressing cells (gate β3+ outlined with a *dashed box* in *E*) is shown for cells isolated from LPS- and water-treated WT mice. Data shown are the means ± standard errors, n = 10 individual mouse samples per group. *$P = 0.014$ for LPS- versus water-treated WT mice.

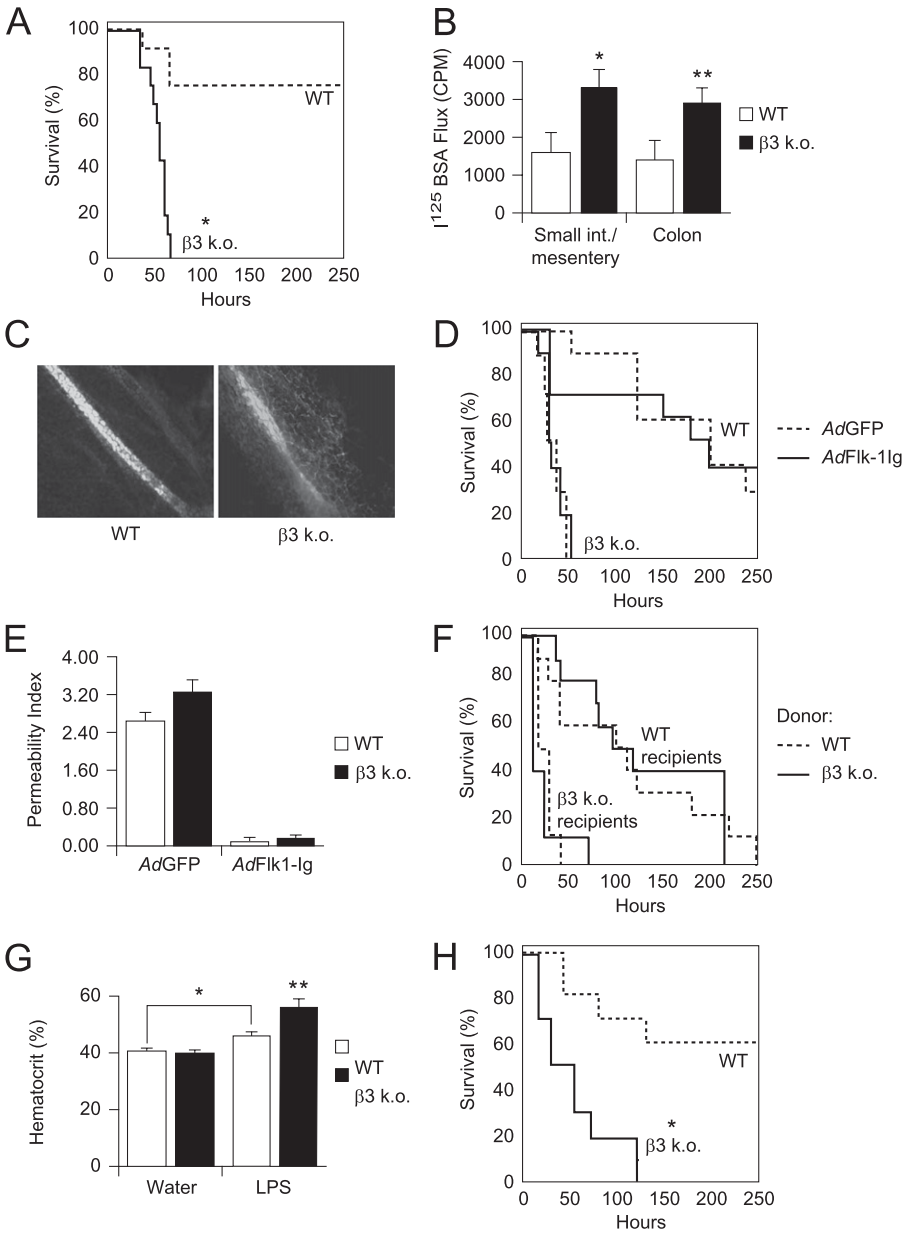

Figure 2. (*A*) β3 knockout (KO) mice have increased mortality after intraperitoneal LPS. LPS was administered to β3 KO and wild-type (WT) control mice by intraperitoneal injection (10 mg/kg). *Solid line* = β3 KO mice, *dashed line* = WT mice. Mortality data analyzed by Kaplan-Meier survival analysis, log-rank test difference between groups, n = 10 mice per group, **P* = 0.0001. (*B*) β3 KO mice have increased vascular leak in small bowel and mesentery and colon after intraperitoneal LPS. LPS was administered to β3 KO and WT control mice by intraperitoneal injection (10 mg/kg). Afterward, an I^{125}–bovine serum albumin (BSA) tracer was administered and the small intestine and mesentery and colon were harvested *en bloc* and analyzed for total counts per minute (CPM). Data shown are the means ± standard errors, n = 6 mice per group. β3 KO versus WT control: **P* = 0.034 for small intestine and mesentery, ***P* = 0.042 for colon. (*C*) β3 KO mice have local vascular leak around mesenteric vessels after intraperitoneal LPS. After intraperitoneal LPS administration (10 mg/kg), fluorescein isothiocyanate–labeled dextran was administered and mesenteric whole mounts were prepared (26). Sites of leakage were identified as areas of local fluorescein isothiocyanate–dextran extravasation. Images were obtained with a ×40 dry objective. (*D*) *In vivo* suppression of vascular endothelial growth factor (VEGF) signaling does affect increased mortality in β3 KO mice after intraperitoneal LPS. Mice infected with adenoviruses expressing a Flk-1–IgG chimera (*Ad*Flk1-Ig) (*solid lines*) or green fluorescent protein (GFP) control (*Ad*GFP) (*dashed lines*) followed by intraperitoneal LPS. Mortality data were analyzed by Kaplan-Meier survival analysis, n = 10 mice per group, log-rank test difference between groups. *P* = 0.670 for β3 KO, *Ad*Flk-1 versus *Ad*GFP; *P* = 0.907 for WT, *Ad*Flk-1 versus *Ad*GFP. (*E*) *Ad*Flk-1 suppresses VEGF-induced dermal vascular leak. After infection with *Ad*Flk1-Ig or *Ad*GFP, response to intradermal VEGF (compared with saline control) was quantified as absorbance units (620 nm) of Evans blue extracted from skin punch biopsies. Data shown are expressed as the Permeability Index = (VEGF site absorbance-saline site absorbance)/saline-site absorbance) ± standard errors, n = 10 mice per group. *P* = 0.053 for *Ad*GFP WT versus β3 KO. (*F*) WT bone marrow engraftment does not rescue early mortality in β3 KO mice after intraperitoneal LPS. Recipient β3 KO and WT mice treated with lethal irradiation were transplanted with bone marrow cells harvested from WT (*dashed lines*) and β3 KO (*solid lines*) mouse donors. After convalescence and confirmation of bone marrow engraftment (*see* Figures E1A and E1B in the online supplement), the mice were administered intraperitoneal LPS (10 mg/kg). Mortality data were analyzed by Kaplan-Meier survival analysis, n = 10 mice per group, log-rank test difference between groups. *P* = 0.608 for WT recipients, WT versus β3 KO donor; *P* = 0.937 for β3 KO recipients, WT versus β3 KO donor. (*G*) β3 KO mice exhibit increased hemoconcentration in LPS-induced sepsis. After intraperitoneal LPS (10 mg/kg) or water control, blood was drawn by inferior venal caval puncture and hematocrit levels measured. Data shown are the means ± standard errors, n = 10 mice per group. **P* = 0.003 for WT versus WT + LPS, ***P* = 0.004 for WT + LPS versus β3 KO + LPS. (*H*) β3 KO mice have increased mortality in cecal ligation and puncture–induced sepsis. β3 KO and WT control mice were treated with cecal ligation and puncture. *Solid line* = β3 KO mice, *dashed line* = WT mice. Mortality data analyzed by Kaplan-Meier survival analysis, log-rank test difference between groups, n = 10 mice per group, **P* = 0.001.

type mice had baseline expression that increased modestly after endotracheal LPS (Figures 1E and 1F).

β3 KO Mice Have Increased Mortality after Intraperitoneal LPS and CLP

β3 KO mice had dramatically increased mortality compared with wild-type mice after intraperitoneal LPS (Figure 2A). Systemic vascular leak, measured by extravasation of an I^{125}-albumin intravascular tracer into organs harvested *en bloc* after intraperitoneal LPS, was also increased in the β3 KO mice (Figure 2B). Furthermore, extravasation of a FITC-dextran intravascular tracer was detected in the interstitium around mesenteric blood vessels in β3 KO mice, but not in wild-type controls (Figure 2C).

To examine the potential contribution of VEGF signaling (18, 19) to increased intraperitoneal LPS-induced mortality in β3 KO

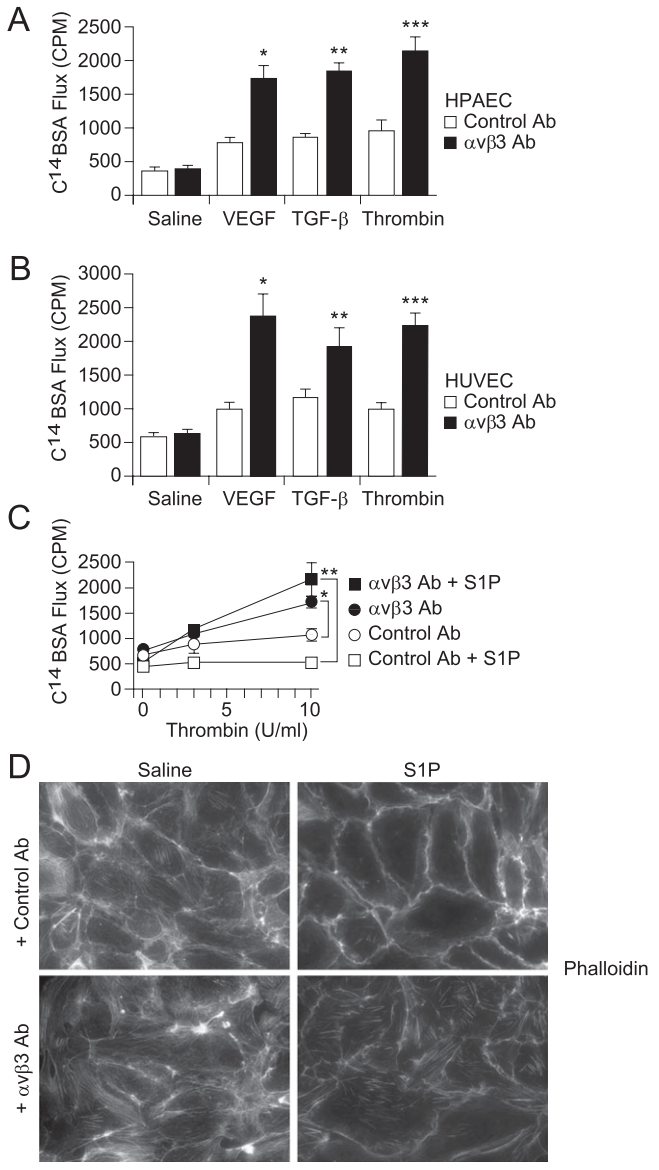

Figure 3. (*A* and *B*) αvβ3 antibodies increase the endothelial permeability response to inflammatory agonists. Serum-starved confluent human pulmonary artery endothelial cell (HPAEC) (*A*) and human umbilical vein endothelial cell (HUVEC) (*B*) monolayers were incubated with αvβ3 or control antibodies (Ab) (10 μg/ml, 1 h) before stimulation with vascular endothelial growth factor (VEGF) (30 ng/ml, 10 min), transforming growth factor (TGF)-β (10 ng/ml, 10 min), or thrombin (10 U/ml, 5 min). C^{14}–bovine serum albumin (BSA) flux across monolayers was measured as counts per minute (CPM) from media collected from basolateral wells. (*A*) HPAECs: Data shown are the means ± standard errors, n = 4 samples per group. Control versus αvβ3 Ab: $P = 0.736$ for saline, $^{*}P = 0.001$ for VEGF, $^{**}P = 0.001$ for TGF-β, $^{***}P = 0.001$ for thrombin. (*B*) HUVECs: Data shown are the means ± standard errors, n = 4 for each group. Control versus αvβ3 Ab: $P = 0.612$ for saline, $^{*}P = 0.002$ for VEGF, $^{**}P = 0.032$ for TGF-β, $^{***}P = 0.002$ for thrombin. (*C*) αvβ3 antibodies inhibit sphingosine-1 phosphate (S1P)–induced resistance to increased permeability effects of thrombin. Serum-starved confluent HPAEC monolayers were incubated with αvβ3 or isotype control antibodies (10 μg/ml, 1 h) before stimulation with S1P (0.5 μM, 5 min) or thrombin (10 U/ml, 5 min). C^{14}-BSA flux across monolayers was measured as CPM collected into basolateral wells. Data shown are the means ± standard errors, n = 4 samples per group. $^{*}P = 0.0006$ for thrombin-treated: control versus αvβ3 Ab. $^{**}P = 0.0007$ for S1P- and thrombin-treated: control versus αvβ3 Ab. (*D*) αvβ3 antibodies disrupt S1P-induced cortical actin in favor of stress fiber formation. Confluent monolayers of HPAECs were pretreated with control or αvβ3 antibodies, then stimulated with S1P or saline control. Cells were then fixed, permeabilized, and stained with rhodamine-phalloidin. Images were acquired with a ×40 dry objective.

mice the effects of *in vivo* blockade of VEGF were evaluated. Mice were infected with an adenovirus expressing a soluble Flk-1–IgG chimera designed to scavenge intravascular VEGF. Expression of the Flk-1–IgG chimera did not rescue β3 KO mice from early mortality, nor did it prolong survival time in wild-type mice after intraperitoneal LPS (Figure 2D). Effective VEGF blockade after infection with *Ad*Flk-1–Ig was demonstrated using a dermal vascular leak assay (Figure 2E). These results, together with findings of equivalent Flk-1 expression in β3 KO and wild-type lung endothelial cells (Figures 1C and 1D), suggest that increased vascular leak and mortality in β3 KO mice after endotracheal and intraperitoneal LPS are not explained by amplified effects of VEGF.

The integrin β3 subunit pairs with both αv and αIIb subunits. αIIbβ3, the major integrin expressed on platelets, regulates platelet activation, aggregation, and function. β3 is also expressed on macrophages (32). To address confounding effects of β3 deficiency in platelets and macrophages, mortality after intraperitoneal LPS was measured in β3 KO mice engrafted with wild-type bone marrow. Although all experimental groups had earlier mortality compared with nontransplanted mice (as shown in Figure 2A), which might reflect effects from total body irradiation or engraftment, there was no mortality rescue in β3 KO mice engrafted with wild-type donor marrow, nor earlier mortality in wild-type mice engrafted with β3 KO donor marrow (Figure 2F). Complete bone marrow reconstitution for each mouse was confirmed by measuring β3 expression on platelets isolated after engraftment (*see* Figures E1A and E1B in the online supplement). These results suggest that β3 deficiency in platelets and other hematopoietic cells was not a significant contributor to the early mortality seen in β3 KO mice.

Increased vascular leak typically leads to hemoconcentration, a result of preferential extravasation of fluid from the vasculature and retained circulating red blood cells. In contrast, hemorrhage, a potential consequence of platelet dysfunction, results in anemia and hemodilution. β3 KO mice exhibited increased hemoconcentration in response to intraperitoneal LPS compared with wild-type controls (Figure 2G). These results support the conclusion that an increase in vascular leak, rather than hemorrhage, was associated with the early mortality observed in β3 KO mice.

We next examined the effect of β3 deficiency in a model of CLP. CLP is an experimental model for sepsis induced by polymicrobial peritonitis (33). β3 KO mice had increased mortality compared with wild-type mice after CLP (Figure 2H), corroborating our findings with intraperitoneal LPS (Figure 2A).

αvβ3 Antibodies Produce a Hyperpermeable Response to Multiple Edemagenic Agonists and Overcome Barrier-enhancing Effects of S1P on Endothelial Monolayers

We directly examined the functional role of αvβ3 in regulating endothelial permeability by treating monolayers of human pulmonary artery endothelial cells (HPAECs) and human umbilical vein endothelial cells with αvβ3 blocking antibodies followed by stimulation with edemagenic agonists. Monoclonal αvβ3 antibodies were generated and characterized in our laboratory (*see* Figures E2A and E2B). αvβ3 antibodies did not affect baseline monolayer permeability for either cell type, but dramatically augmented their permeability responses to VEGF, TGF-β, and

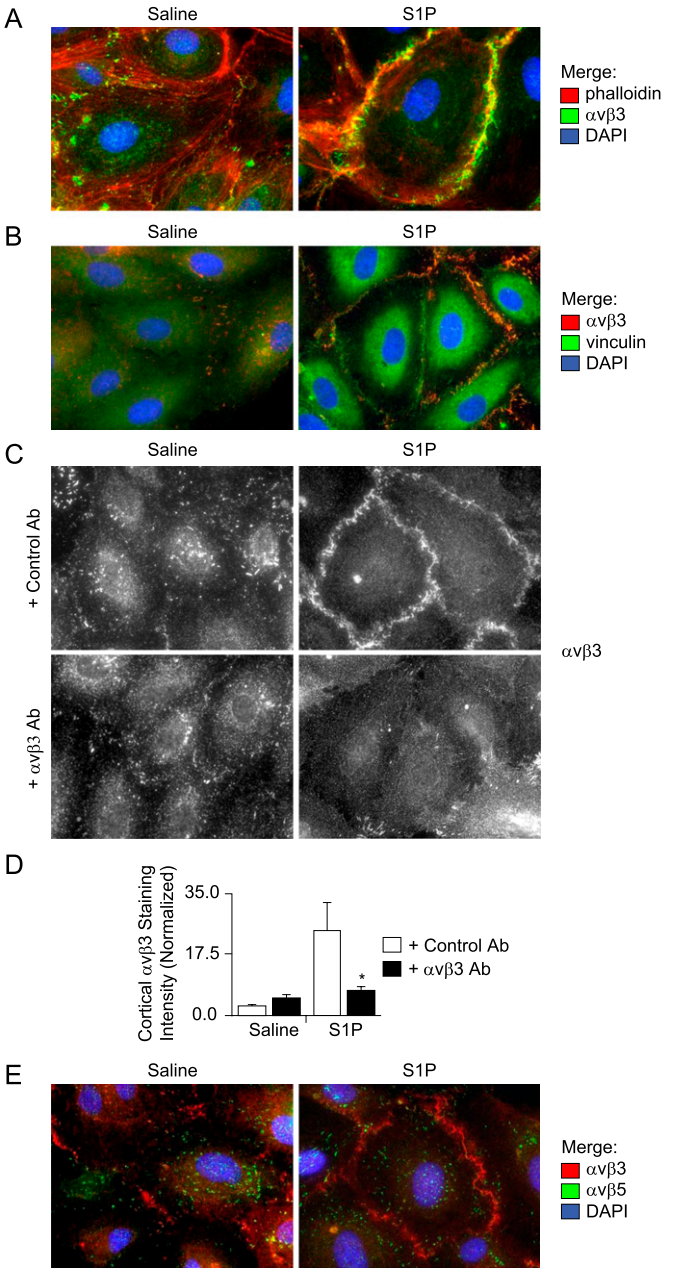

Figure 4. (*A*) Sphingosine-1 phosphate (S1P) induces translocation of αvβ3 to cortical actin sites. Confluent monolayers of human pulmonary artery endothelial cells (HPAECs) were treated with S1P or saline control. Cells were then fixed, permeabilized, and stained with αvβ3 antibodies, rhodamine-phalloidin, and a 4′,6-diamidino-2-phenylindole (DAPI) nuclear stain. Images were pseudocolored *red* for phalloidin, *green* for αvβ3, and *blue* for DAPI. Images were acquired with a ×63 glycerine immersion objective. (*B*) S1P induces colocalization of vinculin and αvβ3 at cortical sites. Confluent monolayers of HPAECs were treated with S1P or saline control. Cells were then fixed, permeabilized, and stained with αvβ3 and vinculin antibodies. Images were acquired with a ×63 glycerine immersion objective. (*C* and *D*) S1P induces translocation of αvβ3 to cortical focal adhesions, which are resolved by total internal reflection fluorescence microscopy and inhibited by αvβ3 antibodies. (*C*) Confluent monolayers of HPAECs were treated with S1P (0.5 μM, 5 min) or saline control. Cells were then fixed, permeabilized, and stained with αvβ3 antibodies. Images obtained using total internal reflection fluorescence imaging with a ×63 oil immersion objective. (*D*) Cortical αvβ3 staining intensity was analyzed by measuring pixel bitmap intensity in areas of interest applied to cortical cell–cell junction sites. Normalized intensity = (mean of maximum pixel intensities per areas of interest)/(minimum field pixel intensity). Minimum field pixel intensity was determined by histogram intensity analysis of each panel field. Data shown are the means ± standard errors, n = 10 panels per group with 40 areas of interest averaged per panel, **P* = 0.0294 for S1P-treated: control versus αvβ3 Ab. (*E*) S1P induces unique translocation of αvβ3. Confluent monolayers of HPAECs were treated with S1P (0.5 μM, 5 min) or saline control. Cells were then fixed, permeabilized, and stained with αvβ3 and αvβ5 antibodies and a DAPI nuclear stain. Images were pseudocolored *red* for αvβ3, *green* for αvβ5, and *blue* for DAPI. Images were acquired with a ×63 glycerine immersion objective.

thrombin (Figures 3A and 3B). VEGF, TGF-β, and thrombin increase endothelial permeability by activating distinct receptor families and proximal signaling pathways (34–37). These results suggest that αvβ3 normally functions to facilitate resistance against increased permeability in both pulmonary and systemic vascular endothelium, and that these effects occur downstream to multiple distinct signaling pathways.

S1P is an endogenous sphingolipid that increases endothelial resistance to permeability and plays an important homeostatic role in preventing exaggerated vascular permeability responses (21, 38, 39). Mice lacking plasma S1P have marked increases in induced permeability, similar to the results described in β3 KO mice (38). The role of αvβ3 in SIP-induced barrier resistance was examined by treating HPAEC monolayers with αvβ3 antibodies, followed by S1P, and then by thrombin (Figure 3C). As expected, S1P inhibited thrombin-induced increases in permeability. αvβ3 antibodies caused a hyperpermeable response to thrombin (as also shown in Figures 3A and 3B), and eliminated S1P-induced resistance to thrombin-induced permeability.

S1P-induced endothelial resistance has been associated with cortical reorganization of cytoskeletal actin (20, 40, 41). αvβ3 antibodies disrupted S1P-induced cortical actin and seemed to simultaneously enhance formation of actin stress fibers (Figure 3D). Stress fiber formation has been implicated in facilitating paracellular gap formation and increased endothelial monolayer permeability (34, 42).

S1P Induces αvβ3 Translocation to Focal Adhesions Located at Peripheral Cortical Actin Sites

S1P induced translocation of αvβ3 from discrete focal adhesions to circumferential clusters colocalized to the cortical actin ring (Figure 4A). These cortical αvβ3 clusters represent peripherally distributed focal adhesions, as demonstrated by colocalization of αvβ3 with vinculin (Figure 4B); vinculin is a membrane-cytoskeletal protein that is known to facilitate both integrin clustering at focal adhesions and linkage to the actin cytoskeleton (43). Furthermore, αvβ3 antibodies attenuated S1P-induced cortical localization of αvβ3 when quantified by cortical cell–cell junction pixel intensity analysis of TIRF images (Figures 4C and 4D); TIRF allows imaging of cell membrane and extracellular cell substrate interactions. These data suggest that αvβ3 ligation is required to stabilize cortically redistributed αvβ3 focal adhesions, and that formation of these focal adhesions is required for S1P-induced cortical actin formation and endothelial barrier enhancement.

Although S1P induced translocation of αvβ3 to cortical sites, it did not induce translocation of αvβ5. αvβ5 is a closely related integrin to αvβ3 that is also expressed on endothelial cells, shares the common αv subunit, and shares the extracellular matrix ligand vitronectin (Figure 4E). These data suggest that S1P-induced translocation of integrin focal adhesions is unique to αvβ3.

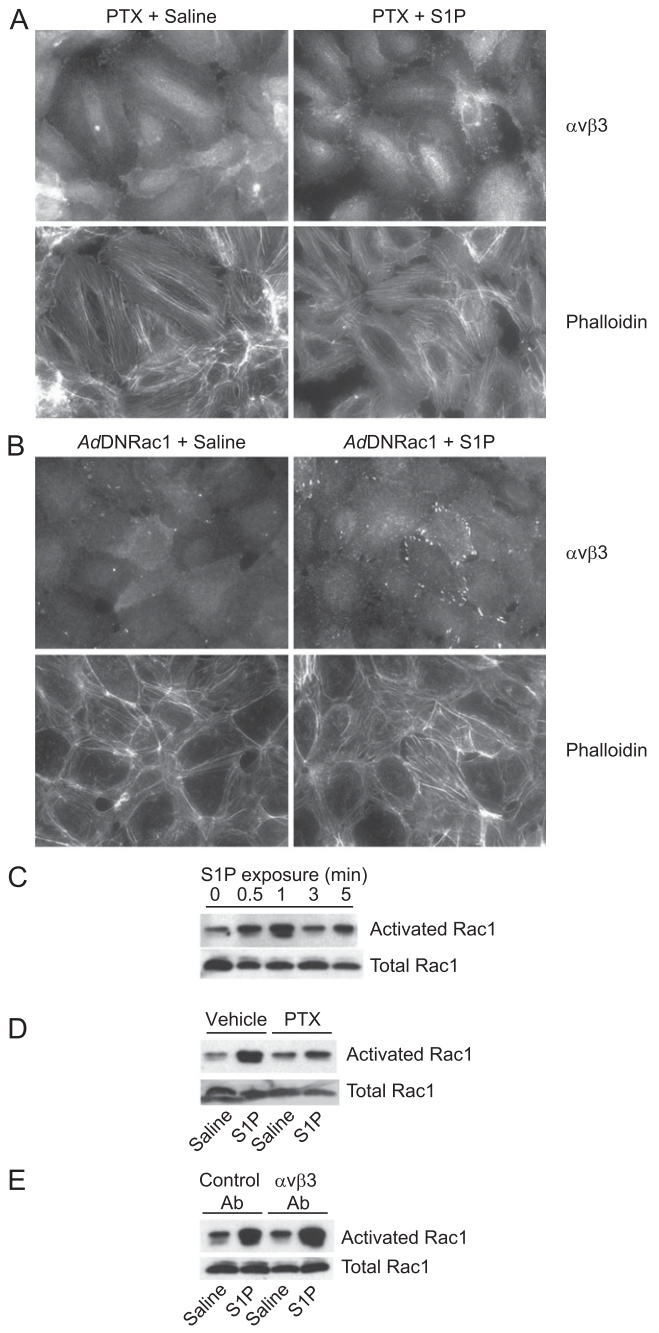

Figure 5. (*A*) Sphingosine-1 phosphate (S1P)–induced cortical translocation of αvβ3 and cortical actin formation are inhibited by pertussis toxin (PTX). Confluent monolayers of human pulmonary endothelial cells (HPAECs) pretreated with PTX (1 μg/ml, 4 h) were treated with S1P (0.5 μM, 5 min) or saline control. Cells were then fixed, permeabilized, and stained with αvβ3 antibodies and rhodamine-phalloidin. Images were acquired with a ×40 dry objective. (*B*) S1P-induced cortical translocation of αvβ3 and cortical actin formation are Rac dependent. HPAECs were infected adenoviruses expressing either a dominant negative Rac1 mutant (N17) (*Ad*DN Rac1) or green fluorescent protein control (*Ad*GFP) (15 multiplicities of infection) (*see* Figure E3). After 48 hours, infected cells were collected and seeded onto glass coverslips coated with 0.1% gelatin. Confluent cells were treated with S1P (0.5 μM, 5 min) or saline control. Cells were then fixed, permeabilized, and stained with αvβ3 antibodies and rhodamine-phalloidin. Images were acquired with a ×40 dry objective. (*C* and *D*) S1P-induced Rac1 activation is inhibited by PTX. (*C*) Cells were treated with saline control of S1P (0.5 μM, 5 min) for designated time points. (*D*) Cells pretreated with PTX (1 μg/ml, 4 h) or vehicle control were treated with S1P or saline control (1-min time point). Activated Rac1 was measured by p21 activated kinase 1 binding domain pulldown from total cell lysates. Samples were Western blotted for Rac1. Loading controls consisted of equivalent volume loading from prepulldown total lysates for each sample. (*E*) S1P-induced Rac1 activation is not inhibited by αvβ3 antibodies. HPAECs pretreated with αvβ3 or control antibodies were treated with S1P (0.5 μM, 5 min) or saline control (1-min time point). Activated Rac1 was measured by total lysate pulldown with beads conjugated with a p21 activated kinase 1 domain that recognizes only guanosine triphosphate–bound active Rac1. Samples were Western blotted for Rac1. Loading controls consisted of equivalent volume loading from prepulldown total lysates for each sample.

S1P-induced Cortical Translocation of αvβ3 and Cortical Actin Formation Are Gi- and Rac1-dependent

S1P-induced endothelial barrier enhancement and cortical actin formation require signaling through the $S1P_1$ receptor by Gi protein coupling (21, 44). Pertussis toxin, which abolishes Gi-dependent signaling through adenosine diphosphate ribosylation of pertussis toxin–sensitive G protein substrates, inhibited αvβ3 translocation to cortical actin sites (Figure 5A).

S1P-induced endothelial barrier enhancement and cortical actin formation have been shown to be dependent on the Rac1 GTPase (21). S1P-induced αvβ3 translocation to cortical sites was inhibited by expression of a dominant negative mutant of Rac1 (Rac N17) (Figure 5B) (green fluorescent protein adenoviral controls shown in Figure E3). In HPAECs, S1P induced a pertussis toxin–sensitive and time-dependent increase in Rac1 activation, with a peak effect at 1 minute (Figures 5C and 5D). αvβ3 antibodies did not affect S1P-induced Rac1 activation (Figure 5E), suggesting that αvβ3 effects occur downstream to Rac1.

DISCUSSION

In this study, β3 KO mice developed striking increases in mortality and systemic vascular leak after intraperitoneal LPS and CLP, and increased lung vascular leak after endotracheal LPS-induced ALI. Bone marrow reconstitution experiments ruled out significant effects caused by β3 deficiency in hematopoietic cells, including platelet activation defects, which may have led to bleeding diathesis and hemorrhage; changes in secretion of vasoactive mediators from hematopoietic cells (including S1P); and alterations in inflammatory cell function (e.g., abnormal neutrophil trafficking) (45). We hypothesized, therefore, that increased susceptibility of β3 KO mice to sepsis mortality and ALI was a manifestation of a vascular endothelial permeability defect.

Previous studies have described increased VEGF-induced dermal vascular permeability in β3 KO mice and attributed this effect to increased VEGF receptor 2 (Flk-1) expression in endothelial cells (18, 19). In our study, *in vivo* blockade of VEGF signaling did not alter mortality after intraperitoneal LPS, nor was Flk-1 expression increased in newly isolated β3 KO endothelial cells. Furthermore, αvβ3 antibodies produced large increases in endothelial permeability in response to edemagenic agonists including TGF-β and thrombin, and VEGF. These data suggest that αvβ3 modulates endothelial permeability through mechanisms downstream to multiple distinct signaling pathways.

S1P is an agonist generated at sites of increased vascular leak and is an important regulator of endothelial permeability and homeostasis *in vivo* (39). We found that αvβ3 antibodies disrupted S1P-induced barrier enhancement and cortical actin formation

in human endothelial cell monolayers. Furthermore, S1P induced unique αvβ3 (compared with αvβ5) translocation to peripheral vinculin-containing structures resolvable by TIRF microscopy, suggesting that αvβ3 is induced by S1P to form cortical focal adhesions. αvβ3 antibodies inhibited formation of these cortical focal adhesions, suggesting that stabilization of these structures requires αvβ3 ligation, and that redistribution of αvβ3-containing focal adhesions is required for S1P-induced cortical actin formation.

S1P-induced αvβ3 translocation occurred through Gi- and Rac1-mediated pathways, which are known to be involved in S1P-induced barrier enhancement and cortical actin formation (21). In this study, we addressed whether αvβ3 effects on the S1P-Rac1 axis could be occurring upstream of or downstream to Rac1 activation. Previous investigations have shown that the activation state of Rac1 and other Rho GTPases can be regulated by integrin ligation state (46–48). These studies also suggest that downstream effects of Rac1 activation, such as activation of Rac1 effectors, may also require effects governed by integrins (47, 48). Therefore, it is possible for integrins to regulate both activation state and downstream effects of Rho GTPases. This paradigm likely varies with different cell types and states (altered integrin ligation) and with different signaling pathways. The current study shows that for human endothelial cell monolayers grown on a stable extracellular matrix, S1P-mediated induction of Rac1 activity is not affected by αvβ3 antibodies, whereas αvβ3 translocation, cortical focal adhesion formation, and cortical actin formation are, suggesting that relevant αvβ3 effects occur downstream of S1P-mediated Rac1 activation.

Several other integrins are expressed in endothelial cells, including αvβ5, α6β4, and multiple β1-contatining integrins (49), so it is surprising that there does not seem to be compensatory support of S1P-induced barrier resistance and cortical actin formation. Furthermore, the apparent specificity of our findings to αvβ3 is of interest. Integrins do not possess intrinsic enzymatic or actin-binding activity; therefore, specificity of their regulatory functions depends largely on interactions with additional cytoplasmic or transmembrane partners. Identification of αvβ3-interacting proteins that facilitate SIP-signaling, promote αvβ3 translocation and stabilization, form and stabilize cortical actin, and function as Rac1 effector targets would provide valuable clues to the mechanisms underlying these processes and would help explain how functional specificity is conferred to αvβ3.

Vinculin, which was found to colocalize with cortical αvβ3 in response to S1P, does not directly bind to integrins, but is thought to support focal adhesion assembly by indirectly coupling talin and α-actinin to the actin cytoskeleton and by recruiting additional proteins, such as paxillin and vinexin (50). Therefore, vinculin could theoretically facilitate formation of cortical αvβ3-containing focal adhesions and participate in stabilization of cortical actin. However, because activated vinculin binds to talin (51, 52), which promiscuously binds to multiple integrin β subunit cytoplasmic domains (53), it seems unlikely that vinculin itself could confer specific of the observed effects to αvβ3.

In conclusion, we have identified αvβ3 as a unique integrin regulator of barrier resistance in the vascular endothelium. αvβ3 is not thought to regulate normal blood vessel development and function (18, 54, 55) (male β3 KO mice have abnormal development of coronary capillaries [56]; our experiments used female mice exclusively); however, our study suggests that loss or functional blockade of αvβ3 results in uncompensated vascular leak in inflammatory states. Novel mechanisms that may be associated with this function include S1P-induced translocation of αvβ3 to cortical focal adhesion sites and stabilization of these cortical focal adhesions through ligation of αvβ3. Elucidation of underlying mechanistic details would provide valuable insights into how αvβ3 and perhaps other integrins modulate endothelial barrier function in response to inflammation, and thus identify novel therapeutic targets to treat pathologic vascular endothelial permeability.

To the extent that endotracheal and intraperitoneal LPS and CLP can adequately model human ALI and sepsis, our results suggest that functional blockade of αvβ3 in humans may produce increased susceptibility to vascular permeability and its associated consequences in these disease states. Drugs designed to block αvβ3 are currently in various stages of clinical trials as treatments for diseases including postmenopausal osteoporosis, rheumatoid arthritis, and cancer. Our results, therefore, suggest that increased intensity of vascular endothelial leak in the setting of sepsis and ALI may be an important undesirable consequence of otherwise promising αvβ3-targeted therapies.

Author disclosures are available with the text of this article at www.atsjournals.org.

Acknowledgment: The authors thank Kurt Thorn and Alice Thwin for their assistance with total internal reflection fluorescence imaging, and also thank Jianlong Lou for his characterization of αvβ3 antibodies.

References

1. Rubenfeld GD, Caldwell E, Peabody E, Weaver J, Martin DP, Neff M, Stern EJ, Hudson LD. Incidence and outcomes of acute lung injury. *N Engl J Med* 2005;353:1685–1693.
2. Martin GS, Mannino DM, Eaton S, Moss M. The epidemiology of sepsis in the United States from 1979 through 2000. *N Engl J Med* 2003;348: 1546–1554.
3. Rubenfeld GD. Epidemiology of acute lung injury. *Crit Care Med* 2003; 31:S276–S284.
4. Ware LB, Matthay MA. The acute respiratory distress syndrome. *N Engl J Med* 2000;342:1334–1349.
5. Deng X, Wang X, Andersson R. Endothelial barrier resistance in multiple organs after septic and nonseptic challenges in the rat. *J Appl Physiol* 1995;78:2052–2061.
6. Groeneveld AB. Vascular pharmacology of acute lung injury and acute respiratory distress syndrome. *Vascul Pharmacol* 2002;39:247–256.
7. Mura M, dos Santos CC, Stewart D, Liu M. Vascular endothelial growth factor and related molecules in acute lung injury. *J Appl Physiol* 2004; 97:1605–1617.
8. Garcia JG, Davis HW, Patterson CE. Regulation of endothelial cell gap formation and barrier dysfunction: role of myosin light chain phosphorylation. *J Cell Physiol* 1995;163:510–522.
9. Lum H, Malik AB. Regulation of vascular endothelial barrier function. *Am J Physiol* 1994;267:L223–L241.
10. Dudek SM, Garcia JG. Cytoskeletal regulation of pulmonary vascular permeability. *J Appl Physiol* 2001;91:1487–1500.
11. Lampugnani MG, Resnati M, Dejana E, Marchisio PC. The role of integrins in the maintenance of endothelial monolayer integrity. *J Cell Biol* 1991;112:479–490.
12. Eliceiri BP, Puente XS, Hood JD, Stupack DG, Schlaepfer DD, Huang XZ, Sheppard D, Cheresh DA. Src-mediated coupling of focal adhesion kinase to integrin alpha(v)beta5 in vascular endothelial growth factor signaling. *J Cell Biol* 2002;157:149–160.
13. Su G, Hodnett M, Wu N, Atakilit A, Kosinski C, Godzich M, Huang XZ, Kim JK, Frank JA, Matthay MA, *et al*. Integrin alphavbeta5 regulates lung vascular permeability and pulmonary endothelial barrier function. *Am J Respir Cell Mol Biol* 2007;36:377–386.
14. Luscinskas FW, Lawler J. Integrins as dynamic regulators of vascular function. *FASEB J* 1994;8:929–938.
15. Hynes RO. Integrins: versatility, modulation, and signaling in cell adhesion. *Cell* 1992;69:11–25.
16. Qiao RL, Yan W, Lum H, Malik AB. Arg-Gly-Asp peptide increases endothelial hydraulic conductivity: comparison with thrombin response. *Am J Physiol* 1995;269:C110–C117.
17. Wu MH, Ustinova E, Granger HJ. Integrin binding to fibronectin and vitronectin maintains the barrier function of isolated porcine coronary venules. *J Physiol* 2001;532:785–791.

18. Robinson SD, Reynolds LE, Wyder L, Hicklin DJ, Hodivala-Dilke KM. Beta3-integrin regulates vascular endothelial growth factor-A-dependent permeability. *Arterioscler Thromb Vasc Biol* 2004;24:2108–2114.
19. Reynolds AR, Reynolds LE, Nagel TE, Lively JC, Robinson SD, Hicklin DJ, Bodary SC, Hodivala-Dilke KM. Elevated Flk1 (vascular endothelial growth factor receptor 2) signaling mediates enhanced angiogenesis in beta3-integrin-deficient mice. *Cancer Res* 2004;64:8643–8650.
20. Dudek SM, Jacobson JR, Chiang ET, Birukov KG, Wang P, Zhan X, Garcia JG. Pulmonary endothelial cell barrier enhancement by sphingosine 1-phosphate: roles for cortactin and myosin light chain kinase. *J Biol Chem* 2004;279:24692–24700.
21. Garcia JG, Liu F, Verin AD, Birukova A, Dechert MA, Gerthoffer WT, Bamberg JR, English D. Sphingosine 1-phosphate promotes endothelial cell barrier integrity by Edg-dependent cytoskeletal rearrangement. *J Clin Invest* 2001;108:689–701.
22. McVerry BJ, Peng X, Hassoun PM, Sammani S, Simon BA, Garcia JG. Sphingosine 1-phosphate reduces vascular leak in murine and canine models of acute lung injury. *Am J Respir Crit Care Med* 2004;170:987–993.
23. Peng X, Hassoun PM, Sammani S, McVerry BJ, Burne MJ, Rabb H, Pearse D, Tuder RM, Garcia JG. Protective effects of sphingosine 1-phosphate in murine endotoxin-induced inflammatory lung injury. *Am J Respir Crit Care Med* 2004;169:1245–1251.
24. Lee MJ, Van Brocklyn JR, Thangada S, Liu CH, Hand AR, Menzeleev R, Spiegel S, Hla T. Sphingosine-1-phosphate as a ligand for the G protein-coupled receptor EDG-1. *Science* 1998;279:1552–1555.
25. Paik JH, Chae S, Lee MJ, Thangada S, Hla T. Sphingosine 1-phosphate-induced endothelial cell migration requires the expression of EDG-1 and EDG-3 receptors and Rho-dependent activation of alpha vbeta3- and beta1-containing integrins. *J Biol Chem* 2001;276:11830–11837.
26. Baluk P, Thurston G, Murphy TJ, Bunnett NW, McDonald DM. Neurogenic plasma leakage in mouse airways. *Br J Pharmacol* 1999;126: 522–528.
27. Rittirsch D, Huber-Lang MS, Flierl MA, Ward PA. Immunodesign of experimental sepsis by cecal ligation and puncture. *Nat Protoc* 2009;4: 31–36.
28. Rojas M, Woods CR, Mora AL, Xu J, Brigham KL. Endotoxin-induced lung injury in mice: structural, functional, and biochemical responses. *Am J Physiol Lung Cell Mol Physiol* 2005;288:L333–L341.
29. Sepp NT, Li LJ, Lee KH, Brown EJ, Caughman SW, Lawley TJ, Swerlick RA. Basic fibroblast growth factor increases expression of the alpha v beta 3 integrin complex on human microvascular endothelial cells. *J Invest Dermatol* 1994;103:295–299.
30. Max R, Gerritsen RR, Nooijen PT, Goodman SL, Sutter A, Keilholz U, Ruiter DJ, De Waal RM. Immunohistochemical analysis of integrin alpha vbeta3 expression on tumor-associated vessels of human carcinomas. *Int J Cancer* 1997;71:320–324.
31. Singh B, Fu C, Bhattacharya J. Vascular expression of the alpha(v)beta (3)-integrin in lung and other organs. *Am J Physiol Lung Cell Mol Physiol* 2000;278:L217–L226.
32. Savill J, Dransfield I, Hogg N, Haslett C. Vitronectin receptor-mediated phagocytosis of cells undergoing apoptosis. *Nature* 1990;343:170–173.
33. Jaganathan BG, Ruester B, Dressel L, Stein S, Grez M, Seifried E, Henschler R. Rho inhibition induces migration of mesenchymal stromal cells. *Stem Cells* 2007;25:1966–1974.
34. Garcia JG, Siflinger-Birnboim A, Bizios R, Del Vecchio PJ, Fenton JW II, Malik AB. Thrombin-induced increase in albumin permeability across the endothelium. *J Cell Physiol* 1986;128:96–104.
35. van Nieuw Amerongen GP, van Delft S, Vermeer MA, Collard JG, van Hinsbergh VW. Activation of RhoA by thrombin in endothelial hyperpermeability: role of Rho kinase and protein tyrosine kinases. *Circ Res* 2000;87:335–340.
36. Eliceiri BP, Paul R, Schwartzberg PL, Hood JD, Leng J, Cheresh DA. Selective requirement for Src kinases during VEGF-induced angiogenesis and vascular permeability. *Mol Cell* 1999;4:915–924.
37. Clements RT, Minnear FL, Singer HA, Keller RS, Vincent PA. RhoA and Rho-kinase dependent and independent signals mediate TGF-beta-induced pulmonary endothelial cytoskeletal reorganization and permeability. *Am J Physiol Lung Cell Mol Physiol* 2005;288:L294–L306.
38. Camerer E, Regard JB, Cornelissen I, Srinivasan Y, Duong DN, Palmer D, Pham TH, Wong JS, Pappu R, Coughlin SR. Sphingosine-1-phosphate in the plasma compartment regulates basal and inflammation-induced vascular leak in mice. *J Clin Invest* 2009;119:1871–1879.
39. Tauseef M, Kini V, Knezevic N, Brannan M, Ramchandaran R, Fyrst H, Saba J, Vogel SM, Malik AB, Mehta D. Activation of sphingosine kinase-1 reverses the increase in lung vascular permeability through sphingosine-1-phosphate receptor signaling in endothelial cells. *Circ Res* 2008;103:1164–1172.
40. Singleton PA, Dudek SM, Chiang ET, Garcia JG. Regulation of sphingosine 1-phosphate-induced endothelial cytoskeletal rearrangement and barrier enhancement by S1P1 receptor, PI3 kinase, Tiam1/Rac1, and alpha-actinin. *FASEB J* 2005;19:1646–1656.
41. Shikata Y, Birukov KG, Birukova AA, Verin A, Garcia JG. Involvement of site-specific FAK phosphorylation in sphingosine-1 phosphate- and thrombin-induced focal adhesion remodeling: role of Src and GIT. *FASEB J* 2003;17:2240–2249.
42. Garcia JG, Verin AD, Schaphorst K, Siddiqui R, Patterson CE, Csortos C, Natarajan V. Regulation of endothelial cell myosin light chain kinase by Rho, cortactin, and p60(src). *Am J Physiol* 1999;276:L989–L998.
43. Humphries JD, Wang P, Streuli C, Geiger B, Humphries MJ, Ballestrem C. Vinculin controls focal adhesion formation by direct interactions with talin and actin. *J Cell Biol* 2007;179:1043–1057.
44. Liu F, Verin AD, Wang P, Day R, Wersto RP, Chrest FJ, English DK, Garcia JG. Differential regulation of sphingosine-1-phosphate- and VEGF-induced endothelial cell chemotaxis. Involvement of G(ialpha2)-linked Rho kinase activity. *Am J Respir Cell Mol Biol* 2001;24:711–719.
45. Watanabe S, Mukaida N, Ikeda N, Akiyama M, Harada A, Nakanishi I, Nariuchi H, Watanabe Y, Matsushima K. Prevention of endotoxin shock by an antibody against leukocyte integrin beta 2 through inhibiting production and action of TNF. *Int Immunol* 1995;7:1037–1046.
46. Price LS, Leng J, Schwartz MA, Bokoch GM. Activation of Rac and Cdc42 by integrins mediates cell spreading. *Mol Biol Cell* 1998;9: 1863–1871.
47. del Pozo MA, Price LS, Alderson NB, Ren XD, Schwartz MA. Adhesion to the extracellular matrix regulates the coupling of the small GTPase Rac to its effector PAK. *EMBO J* 2000;19:2008–2014.
48. Del Pozo MA, Kiosses WB, Alderson NB, Meller N, Hahn KM, Schwartz MA. Integrins regulate GTP-Rac localized effector interactions through dissociation of Rho-GDI. *Nat Cell Biol* 2002;4:232–239.
49. Stupack DG, Cheresh DA. ECM remodeling regulates angiogenesis: endothelial integrins look for new ligands. *Sci STKE* 2002;2002:PE7.
50. Ziegler WH, Liddington RC, Critchley DR. The structure and regulation of vinculin. *Trends Cell Biol* 2006;16:453–460.
51. Gingras AR, Vogel KP, Steinhoff HJ, Ziegler WH, Patel B, Emsley J, Critchley DR, Roberts GC, Barsukov IL. Structural and dynamic characterization of a vinculin binding site in the talin rod. *Biochemistry* 2006;45:1805–1817.
52. Papagrigoriou E, Gingras AR, Barsukov IL, Bate N, Fillingham IJ, Patel B, Frank R, Ziegler WH, Roberts GC, Critchley DR, *et al*. Activation of a vinculin-binding site in the talin rod involves rearrangement of a five-helix bundle. *EMBO J* 2004;23:2942–2951.
53. Gingras AR, Ziegler WH, Bobkov AA, Joyce MG, Fasci D, Himmel M, Rothemund S, Ritter A, Grossmann JG, Patel B, *et al*. Structural determinants of integrin binding to the talin rod. *J Biol Chem* 2009; 284:8866–8876.
54. Hodivala-Dilke KM, McHugh KP, Tsakiris DA, Rayburn H, Crowley D, Ullman-Cullere M, Ross FP, Coller BS, Teitelbaum S, Hynes RO. Beta3-integrin-deficient mice are a model for Glanzmann thrombasthenia showing placental defects and reduced survival. *J Clin Invest* 1999;103:229–238.
55. Reynolds LE, Wyder L, Lively JC, Taverna D, Robinson SD, Huang X, Sheppard D, Hynes RO, Hodivala-Dilke KM. Enhanced pathological angiogenesis in mice lacking beta3 integrin or beta3 and beta5 integrins. *Nat Med* 2002;8:27–34.
56. Weis SM, Lindquist JN, Barnes LA, Lutu-Fuga KM, Cui J, Wood MR, Cheresh DA. Cooperation between VEGF and beta3 integrin during cardiac vascular development. *Blood* 2007;109:1962–1970.